Nuclear charge radii in modern mass formulas

F. Buchinger and J. E. Crawford
Foster Radiation Laboratory, McGill University, 3610 University Street, Montréal, Québec, Canada H3A 2B2

A. K. Dutta
Laboratoire de Physique Nucléaire, Université de Montréal, Montréal, Québec, Canada H3C 3J7
and School of Physics, Devi Ahilya University, Indore, 452001 India

J. M. Pearson
Laboratoire de Physique Nucléaire, Université de Montréal, Montréal, Québec, Canada H3C 3J7

F. Tondeur
Institut d'Astronomie et d'Astrophysique, Université Libre de Bruxelles,
and Institut Supérieur Industriel de Bruxelles, Brussels, Belgium
(Received 6 August 1993)

We examine the predictions for nuclear charge radii made by an extended Thomas-Fermi mass formula, the first to be built entirely on microscopic forces, and the finite-range droplet model mass formula, the most refined of the droplet-model approaches. The former is highly successful, the parameters emerging from the mass fit giving an optimal fit to charge radii also, without any further adjustment. The latter model in its published form seems to suffer from an inappropriate choice for the values of some of the parameters, and we discuss how improvement might be possible.

PACS number(s): 21.10.Dr, 21.30.+y, 21.60.Jz, 21.10.Ft

I. INTRODUCTION

A considerable effort continues to be devoted to the measurement and study of nuclear charge radii. Their systematics reveal several significant aspects of nuclear structure, and in particular they constitute the main source of information concerning the density of nuclear matter. Thus, in this latter respect, the study of nuclear radii can serve to impose strong constraints on the saturation properties of nuclear forces, a point of considerable significance not only for nuclear theory, but also for the understanding of stellar collapse and type II supernova explosions.

Charge-radius systematics also display structural effects related to nuclear shape transitions, providing information that is often complementary to that given by nuclear spectroscopy. In this way, they contribute to our detailed knowledge of the shell strucure of nuclei, thus providing constraints on mean-field theories of the nucleus.

Finally, charge radii and, more generally, charge-density distributions provide direct information on the Coulomb energy of nuclei, and are thus of great interest for the so-called nuclear mass formulas. It is with this aspect that we shall be concerned in this paper.

Although nearly 60 years have elapsed since Bethe and von Weizsäcker proposed their famous formula, a considerable effort continues to be devoted to the development of ever more sophisticated nuclear mass formulas. Much of the motivation for this effort lies in the fact that the late stages of stellar nucleosynthesis, particularly the so-called r process, depend crucially on the binding energies (among other properties) of nuclei so neutron rich that there is no possibility of being able to measure them in the laboratory. It is thus of the greatest importance to be able to make reliable extrapolations of masses (and other properties) away from the known region, relatively close to the stability line, out towards the neutron-drip line.

Modern mass formulas no longer take the form of simple algebraic expressions, as was the case until some 30 years ago. Rather, they are fully fledged nuclear models of considerable sophistication, taking into account shell structure, pairing effects and deformability. As such, they make predictions for other properties besides masses, such as charge and matter distributions, fission barriers, and single-particle (s.p.) wave functions. How well these models can reproduce the experimental charge distributions constitutes a crucial test for their validity.

Until very recently all mass formulas used some form or other of the drop(-let) model of the nucleus to represent the macroscopic, i.e., the smoothly varying part of the nuclear binding energy, and added microscopic corrections to take account of shell and pairing effects. The latest and most refined form of this approach to be published, the so-called finite-range droplet model (FRDM), fits 1593 mass-data points with an rms error of 0.769 MeV in its 1988 version [1], some 25 parameters being used. Since then an improved version which achieves an rms error of only 0.669 MeV for 1654 mass-data points has been announced [2].

However, in the last few years a high-speed approximation to the Hartree-Fock (HF) method has been developed, leading for the first time to the construction of

 ©1994 The American Physical Society

a complete nuclear mass table based entirely on microscopic effective forces [3–6]. This so-called ETFSI approach calculates the macroscopic part of the binding energy in the extended Thomas-Fermi (ETF) approximation, and the shell correction using the Strutinsky theorem in its integral form (SI). Pairing is also taken into account with a δ-function force, handled in the usual way by the BCS method. Although this is still strictly speaking a microscopic-macroscopic model, there is a much greater coherence between the two parts than is the case with mass formulas based on the drop(-let) model, since the same Skyrme force underlies both parts (see Sec. II). This presumably accounts for the fact that with just nine parameters the ETFSI-1 mass formula gives almost as good a fit to the mass data as does the FRDM mass formula, 1492 nuclear masses being fitted with an rms error of 0.736 MeV (parameter set SkSC4 of [6]).

Now it turns out that although the FRDM and ETFSI-1 mass formulas give comparable fits to the mass data they often differ in their extrapolations far from the known region of the nuclear chart. Thus the question arises as to which of the two should be believed. Clearly, one obvious test that any model should satisfy is that of predictability, i.e., new data should be successfully reproduced without any further refitting of the parameters. Both models pass the tests of this kind to which they have been subjected [2, 6], but only because the tests have been made in regions not too far from the stability line, where they agree anyway. Thus the question of which mass formula to believe in those cases of disagreement that are found in the experimentally inaccessible regions remains open.

Generally speaking, one would prefer the formula with the better theoretical foundation, i.e., the one with the better representation of the underlying physics. One indication of the theoretical superiority of one mass formula over another giving a comparable fit to the mass data is that it would achieve this fit with fewer parameters. However, while this criterion should enhance one's confidence in the ETFSI-1 formula at the expense of the FRDM formula, in reality it guarantees nothing, since the form of the Skyrme force underlying the ETFSI-1 model is purely phenomenological, and one could imagine that another model with the same number of parameters would give different extrapolations. Another criterion that could be adopted is to see how well the respective mass formulas predict some nuclear property other than masses, i.e., some property to which the formulas have *not* been fitted.

In this paper we consider such a property, the charge radius, as a test for mass formulas. This is a particularly suitable quantity, since a large amount of precise data has been accumulated over the past decade, even on rare and radioactive isotopes, thanks to the advent of laser spectroscopy [7]. Moreover, the interpretation of the data is relatively straightforward. Specifically, we shall compare the ETFSI and FRDM mass models from this standpoint (for the latter we take the 1988 version [1], the only one to be published so far).

In fact, we shall go beyond the requirement that the mass formulas give *acceptable* radii, and examine the implications of the requirement that for a given model the fits to masses and charge radii should be simultaneously *optimized* by the same parameter set. It is by no means obvious *a priori* that this condition can be satisfied for any given model, and we have here a sensitive test of the internal consistency of the model in question. Furthermore, charge radii may be the most pertinent data for the determination of any of the model parameters that are not unambiguously determined by the masses, as happens in the case of the FRDM.

II. THE MODELS

As a general remark we note that both of the models considered here are of the two-part microscopic-macroscopic type (even if the ETFSI model achieves a very high level of coherence between the two parts), and that the charge radii are determined entirely by the macroscopic part. Both of the present models use the Strutinsky theorem in one form or another to incorporate shell-model corrections into the energy, but these have no *direct* bearing on the density distributions. Nevertheless, in both of the present models the equilibrium deformation that results from the minimization of the *total* energy is strongly influenced by the microscopic terms. Thus to the extent that microscopic effects drive the nuclear deformation they *will* influence the calculated charge radii. But to go further than this in incorporating microscopic effects into the density distributions it is necessary to perform HF calculations, where there is, of course, no separation into macroscopic and microscopic parts.

A. The ETFSI calculation

The ETFSI method has already been described in detail [3–6]. We shall therefore recall here only those aspects relevant to the calculation of charge radii.

In this method the density distributions of protons and neutrons are determined by the ETF part of the calculation, this being the macroscopic part. Rather than determining these distributions by solving the Euler-Lagrange equations, they are parametrized by a suitable functional form, the parameters of which are determined for each nucleus by minimizing the ETF energy calculated for the given Skyrme force. (The same force is then folded over this density distribution to generate the s.p. field that determines the microscopic corrections, thereby ensuring a high level of coherence between the microscopic and macroscopic parts of the model.)

In the limit of spherical nuclei, the functional form assumed *for point nucleons* is the simple Fermi function

$$\rho_q(r) = \frac{\rho_{0q}}{1+\exp(\frac{r-C_q}{a_q})}\ , \tag{1}$$

where q denotes neutrons (n) or protons (p). However, all nuclei are allowed to deform, although the conditions of axial symmetry and left-right symmetry are imposed; deformed configurations are generated from the spherical distribution (1) by means of the (c,h) prescription of Brack *et al.* [8], as described in [4] (note that the parameters C_q and a_q are taken to be deformation independent).

The rms radius of a spherical point-proton distribution of the form (1) is

$$\langle r^2\rangle_p^{1/2} = \sqrt{\frac{3}{5}}C_p\left\{1+\frac{7}{2}\left(\frac{b}{C_p}\right)^2+\cdots\right\} \tag{2}$$

to lowest order in b/C_p, where

$$b = (\pi/\sqrt{3})a_p \tag{3}$$

(see, for example, Myers [9]). As for deformed nuclei, expansions in the multipole deformation parameters are available. However, we prefer to calculate the rms radius essentially exactly by numerical integration over the parametrized proton distribution,

$$\langle r^2\rangle_p = \int \rho(\mathbf{r})r^2 d^3\mathbf{r}. \tag{4}$$

Then folding in the finite proton size, we have for the rms charge radius

$$\langle r^2\rangle_{\rm ch}^{1/2} = \{\langle r^2\rangle_p + s_p^2\}^{1/2}, \tag{5}$$

where $s_p = 0.8$ fm is the rms radius of the proton's charge distribution (see, for example, Eq. (16) of [9], and also the Appendix).

The ETFSI-1 mass table [10], available on request (to J.M.P. or F.T.), gives the rms charge radii of all nuclei with $36 \leq A \leq 300$, calculated as above. All the ETFSI charge radii quoted here come from this table.

Now the rms charge radius is a measure of the lowest moment of the charge distribution, but electron-scattering experiments determine not only this moment but also higher-order moments. Thus, assuming a simple Fermi *charge* (not point-proton) distribution of the form (1), it is possible to measure the diffuseness parameter $a_{\rm ch}$ along with the rms radius, and data compilations give both parameters (also $C_{\rm ch}$, but this is not independent of the other two parameters). To compare with the ETFSI results the value of a_p that emerges from the minimization of the ETF energy has to be corrected for the finite size of the proton. We show how to do this in the Appendix.

B. The FRDM calculation

The 1988 FRDM mass tables of Möller, Myers, Swiatecki, and Treiner (MMST) [1] could have given the charge radii for all nuclei, but did not, and we stress that the charge-radius calculations that we present here are our own. However, the paper of MMST, taken with the earlier paper of Myers and Schmidt (MS) [11], makes the prescription for calculating FRDM charge radii clear and unambiguous, provided the constraints of axial symmetry and left-right symmetry are imposed on the deformation. For all the parameters that appear in the following expressions we take the values given by MMST [1], since these come out of the mass fit of the model (except r_0 and b).

Following Eqs. (21)–(24) of MS, we write for the mean-square radius

$$\langle r^2\rangle_{\rm ch} = \langle r^2\rangle_u + \langle r^2\rangle_r + 3b^2 + s_p^2. \tag{6}$$

The first three terms here are essentially as in Eq. (21) of MS. On the other hand, the last term, representing the finite proton size, as in Eq. (5) for the ETFSI calculation, is new, not, as far as we know, having appeared before in droplet-model calculations *of the radius*. Its presence here is essential, since it appeared in the FRDM mass formula [1], and will thus have affected the values of the other parameters: the value taken in MMST for s_p, and thus here, was 0.8 fm, as in our ETFSI calculations.

As in MS [11], we have for the "uniform" term

$$\langle r^2\rangle_u = \frac{3}{5}R_Z^2 f(\alpha_2,\alpha_4), \tag{7}$$

and for the "Coulomb redistribution" term

$$\langle r^2\rangle_r = \frac{12}{175}C' R_Z^2 g(\alpha_2,\alpha_4), \tag{8}$$

where C' is given by Eq. (17) of MS, and $f(\alpha_2,\alpha_4)$ and $g(\alpha_2,\alpha_4)$ are as in Eqs. (22) and (23), respectively, of MS, with

$$\alpha_l = \sqrt{\frac{2l+1}{4\pi}}\beta_l, \tag{9}$$

where β_l is the multipole deformation tabulated in MMST [1]. The third term of Eq. (6) represents the surface diffuseness, and in the case of a Fermi distribution of the form (1) the parameter b will have the same meaning as in Eq. (3). MMST [1] assume that b takes the same value in all nuclei, but this may not be correct. For example, ETF calculations [3, 5] show that b is indeed A independent to a high degree of accuracy, but does depend on $I = (N-Z)/A$. We do not know whether the approximation of MMST introduces any significant error; in any case they take the constant value $b = 0.99$ fm.

As for the sharp radius R_Z appearing in Eqs. (7) and (8), it is still given by

$$R_Z = R_0\left\{1-\frac{2N}{3A}\frac{I-\bar{\delta}}{B_s}\right\}, \tag{10}$$

with

$$R_0 = r_0 A^{\frac{1}{3}}(1+\bar{\epsilon}) \tag{11}$$

as in MS. However, for $\bar{\epsilon}$ and $\bar{\delta}$ we must now use the expressions of MMST [1], rather than those of MS [11]. The parameter r_0 is the charge-radius constant, related to the saturation density ρ_{00} of symmetric nuclear matter through $\frac{4\pi}{3}r_0^3 = 1/\rho_{00}$. MMST [1] set it equal to 1.16 fm.

III. RESULTS

In comparing the predictions of the two models with experimental values of the charge radius we shall consider both relative values $\delta\langle r^2\rangle$ along an isotopic chain, determined by laser-spectroscopic measurements of isotope shifts, and absolute values, determined by measurements on the elastic scattering of electrons. We recall

that neither model has any free parameters to fit the radius data.

A. Relative charge radii

In Fig. 1 we compare experimental changes of mean-square charge radii for some long isotopic chains to the ETFSI and FRDM calculations. The experimental data were obtained from Ref. [7] and, for more recent data, from Refs. [12–18]. The data displayed cover a major part of the nuclear chart with Z ranging between 20 (Ca) and 88 (Ra), and N varying between 20 and 144. Over the wide range of data considered, the agreement of the predictions from both models with the experimental data is good, on the whole. Actually, it should be noted that for each chain we take the same reference isotope as chosen in the original experimental publication. It then turns out that in some cases the agreement between theory and experiment could be improved by an arbitrary change of the reference isotope, as, for example, in Cd. Here the ETFSI model predicts a shape transition between $N = 64$ and $N = 65$ that does not appear in the experimental data, and it is the resultant error in the calculated radius of the reference nucleus, $N = 66$, that is responsible for the large discrepancies seen in the figure for the light Cd isotopes. With an appropriate change of the reference isotope this discrepancy could be shifted to the far less numerous isotopes with $N > 65$, producing thereby the spurious impression of an improvement.

It should be borne in mind that both calculations contain only static deformations, which are limited to axial symmetry with just even-order multipoles (up to hexadecapole for the FRDM). Thus some of the discrepancies might be due to the absence of dynamic contributions to the deformation, to triaxiality, or to octupole and, probably less important, higher-order multipoles ($l > 5$). This is certainly the case for Ca where the systematic deviations between the models and experimental values are the largest, and where the importance of collective quadrupole and octupole contributions to the deformation has been pointed out on several occasions (see [7] and references therein).

Even though it is not the purpose of this communication to discuss all the presented examples in detail, it is worthwhile to add a few remarks on gross features found in the comparison between the experimental data and the predictions. In both models shell effects are expressed through their influence on the ground state deformation. At $N = 50$ the major shell closure is well expressed in the ETFSI approach (Rb, Sr), whereas the FRDM fails to predict an influence of the shell closure on $\delta\langle r^2_{\rm ch}\rangle$ values. Both models do fairly well for $N = 82$ (Xe, Cs, Ba, Nd, Sm, Eu) in predicting the change in slope of the $\delta\langle r^2_{\rm ch}\rangle$ values, which is not as drastic as observed at $N = 50$. For $N = 126$, neither model indicates any shell effect; however the Pb data still reveal a definite kink, but again less pronounced than at $N = 50$ or 82. The stabilizing effect of the proton shell closure on the nuclear shape is well reproduced by both models in the Sn ($Z = 50$) and Pb ($Z = 82$) region. Here the constant slope of $\delta\langle r^2_{\rm ch}\rangle$ over a wide range of isotopes expresses the change of nuclear volume at constant deformation.

Sharp shape transitions from small to large deformation are correctly predicted in the ETFSI approach for the neutron-rich Rb and Sr isotopes, and for the neutron deficient Hg nuclei. For these cases the FRDM model predicts either no change in deformation (Hg) or a more gradual increase to a final strongly deformed shape (Rb, Sr). Both models fail to predict the sudden increase in deformation observed in the rare-earth region (Eu), favoring a smooth transition from spherical to strongly deformed shape. For Hg the ETFSI approach anticipates a deformation change from small oblate ($\beta_2 = -0.16$) to large prolate ($\beta_2 = 0.45$) for $N = 104$. This is the general trend expected from previous calculations [19, 20] and indicated by the experimental data. However the transition occurs one neutron number lower than expected, the change in deformation is overestimated, and no difference between the ground-state deformation of the odd and even isotopes is found. The corresponding discontinuity in the Hg neighbor Au is not reproduced by either model.

The ETFSI calculations for both Rb and Sr predict too early an onset of deformation for the neutron-rich isotopes. For the neutron-rich Sr isotopes the calculations are remarkably similar to full HF+BCS calculations using force SKa [12]. These calculations reveal the same sharp, but early, onset of deformation and a similar overestimation of $\delta\langle r^2_{\rm ch}\rangle$ for the heaviest isotopes. For the very neutron-deficient isotopes $\delta\langle r^2_{\rm ch}\rangle$ is overestimated in the ETFSI calculations, as in HF calculations with different forces [12, 21]. The FRDM fit is somewhat better for the $\delta\langle r^2_{\rm ch}\rangle$ of the strongly deformed nuclei at both extremes of the Sr chain, with predicted β_2 values which are very similar to those obtained from the ETFSI calculations and to those extracted from experimental $BE2$ values (see Table I). For the transitional proton-rich Rb and Sr isotopes the deficiencies of the FRDM approach have been pointed out on several occasions [12, 24]. In this region the results for $\delta\langle r^2_{\rm ch}\rangle$ from the ETFSI approach are closer to the experimental values.

For the heaviest elements (Rn, Fr, Ra), the agreement of the ETFSI predictions with the data is very good, whereas the FRDM reveals a constant deviation in the

TABLE I. Comparison of the experimental $|\beta_2|$ values for Sr isotopes [22, 23] with the predictions from the ETFSI and FRDM models.

A	ETFSI	FRDM	Expt.
78	0.43	0.41	0.434(27)
80	0.40	0.39	0.377(16)
82	0.30	0.02	0.290(6)
84	0.15	0.03	0.211(5)
86	0.00	0.02	0.128(10)
88	0.00	0.01	0.117(3)
90	0.11	0.04	0.120(19)
92	0.15	0.10	0.116(24)
94	0.19	0.25	0.115(25)
96	0.35	0.34	0.15(4)
98	0.39	0.36	0.409(5)
100	0.38	0.37	0.426(9)

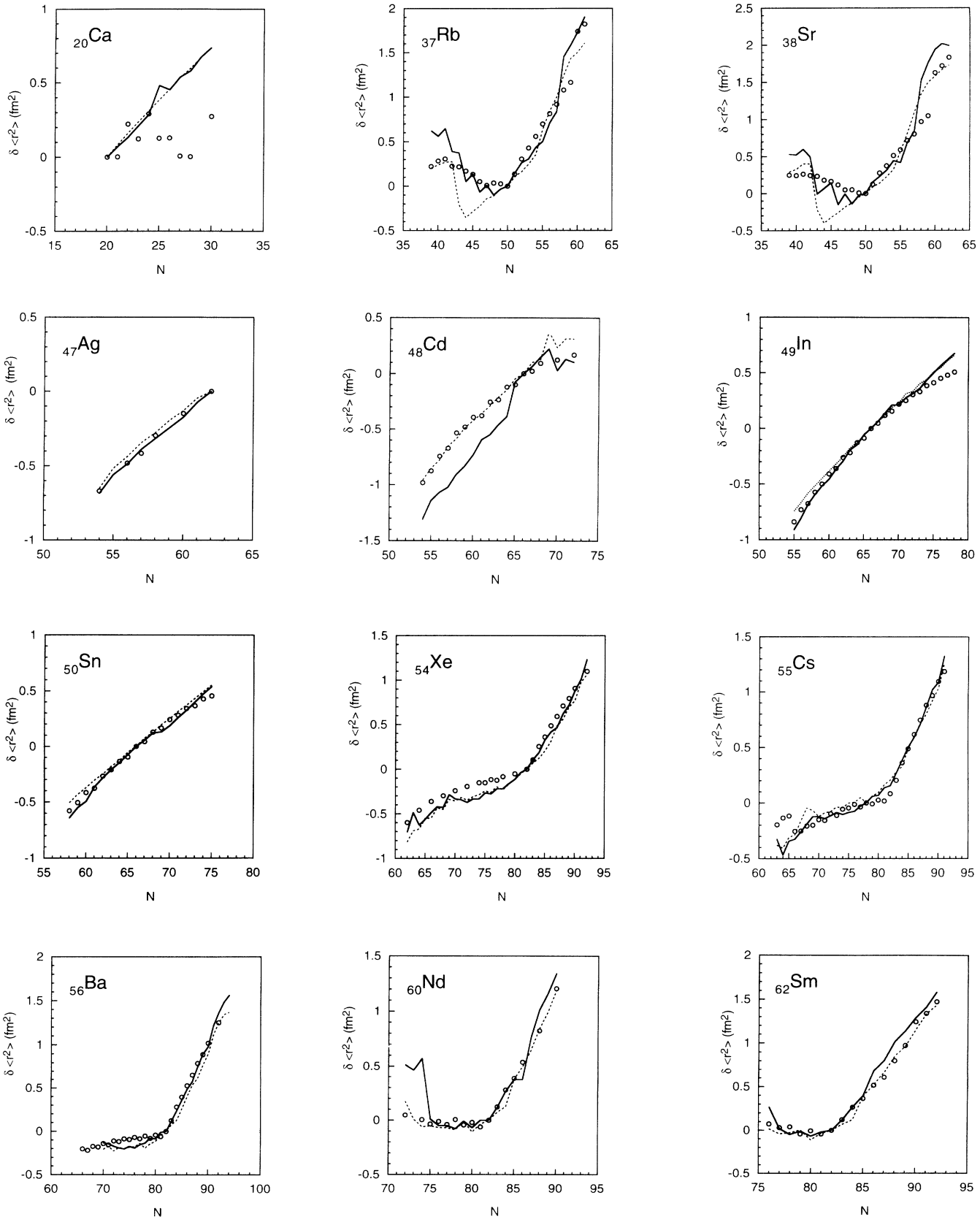

FIG. 1. Comparisons of experimental measurements of change of mean-square charge radius with two theoretical predictions for 24 long isotopic chains. The open circles represent the experimental data points. The ETFSI prediction is shown by the solid line and the FRDM by the dashed line.

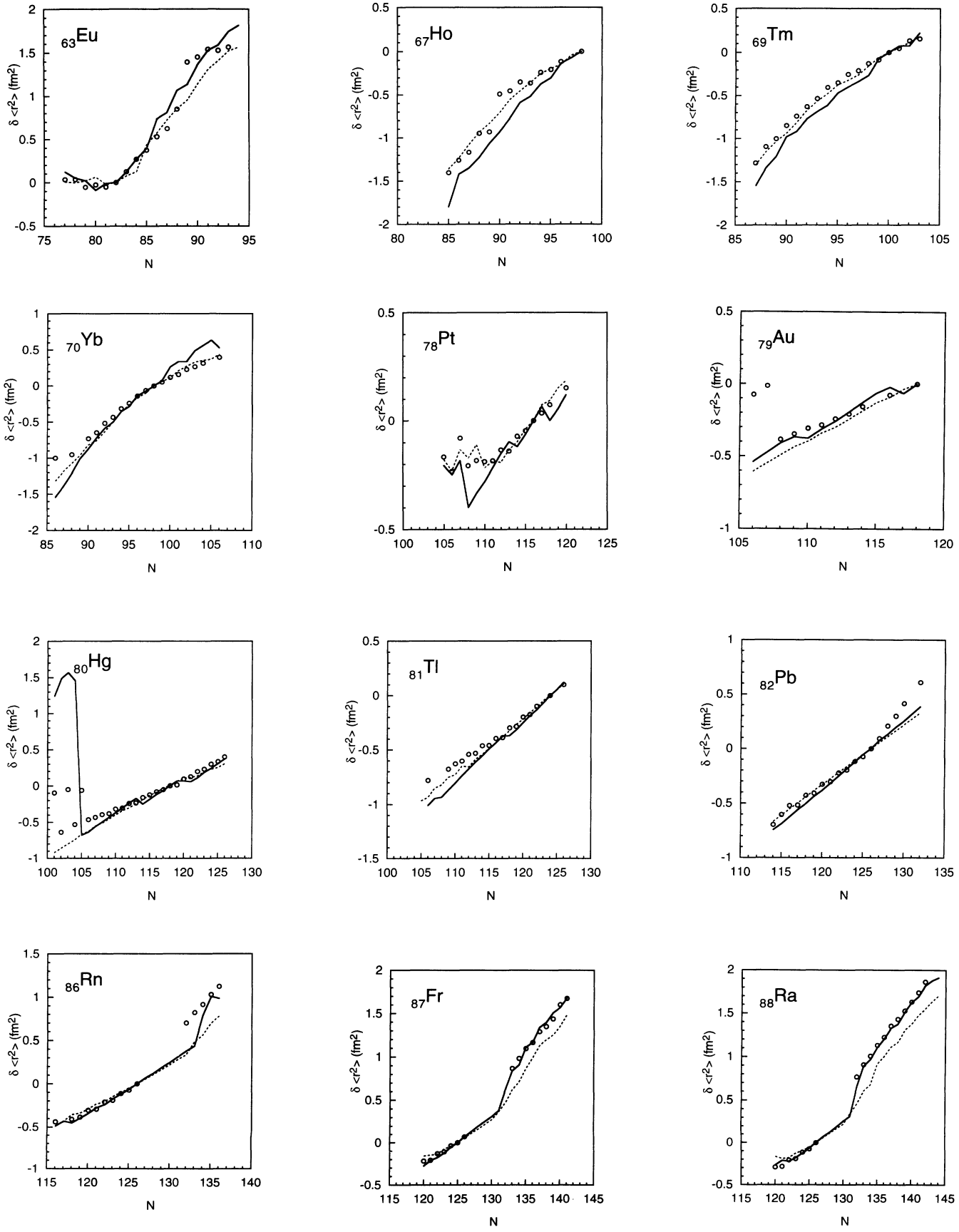

FIG. 1. (*Continued*).

neutron-rich region. It is surprising that the agreement of the ETFSI results is achieved by including only even-order contributions to the deformation since some of the heavy nuclei of these elements are known to exhibit octupole deformation [5, 25, 26]. An inclusion of the octupole degree of freedom into the ETFSI calculations is possible, and it would be interesting to see how much the changes in mean-square charge radii are affected.

One general feature that emerges from these calculations is that the slope of $\delta\langle r^2_{\rm ch}\rangle$ vs N for ETFSI is either comparable to the FRDM slope or greater, i.e., it is somewhat greater on average. This suggests a stronger dilation of the proton distribution by the excess neutrons in ETFSI, which is consistent with the larger value of the surface-stiffness coefficient Q for ETFSI (112.3 MeV [6]) than for FRDM (29.4 MeV [1]). As discussed in [27], the

TABLE II. Absolute rms charge radii (fm).

	ETFSI	FRDM	Expt.		ETFSI	FRDM	Expt.
^{36}S	3.30	3.38	3.28	^{110}Pd	4.58	4.59	4.54
^{37}Cl	3.34	3.42	3.38	^{110}Cd	4.57	4.59	4.58
^{36}Ar	3.40	3.43	3.33	^{112}Cd	4.58	4.61	4.61
^{40}Ar	3.41	3.47	3.42	^{114}Cd	4.64	4.63	4.63
^{39}K	3.42	3.49	3.41	^{116}Cd	4.65	4.64	4.64
^{40}Ca	3.45	3.52	3.45	^{112}Sn	4.59	4.62	4.59
^{48}Ca	3.54	3.60	3.45	^{114}Sn	4.60	4.63	4.60
^{48}Ti	3.60	3.65	3.60	^{116}Sn	4.62	4.64	4.62
^{50}Ti	3.61	3.67	3.57	^{117}Sn	4.62	4.65	4.62
^{51}V	3.64	3.70	3.60	^{118}Sn	4.63	4.66	4.63
^{50}Cr	3.68	3.72	3.66	^{119}Sn	4.63	4.66	4.64
^{52}Cr	3.68	3.73	3.64	^{120}Sn	4.64	4.67	4.64
^{53}Cr	3.69	3.74	3.73	^{122}Sn	4.65	4.68	4.66
^{54}Cr	3.71	3.76	3.69	^{124}Sn	4.67	4.70	4.67
^{55}Mn	3.75	3.79	3.68	^{138}Ba	4.83	4.86	4.85
^{54}Fe	3.74	3.78	3.68	^{139}La	4.85	4.88	4.85
^{56}Fe	3.77	3.81	3.73	^{142}Nd	4.90	4.93	4.92
^{58}Fe	3.78	3.84	3.77	^{144}Nd	4.93	4.94	4.93
^{59}Co	3.81	3.86	3.77	^{146}Nd	4.96	4.98	4.98
^{58}Ni	3.82	3.86	3.77	^{148}Nd	4.99	5.01	5.00
^{60}Ni	3.84	3.88	3.80	^{150}Nd	5.02	5.05	5.01
^{61}Ni	3.84	3.89	3.81	^{144}Sm	4.93	4.96	4.95
^{62}Ni	3.86	3.90	3.83	^{148}Sm	5.00	5.02	4.99
^{64}Ni	3.88	3.92	3.85	^{150}Sm	5.02	5.05	5.04
^{63}Cu	3.89	3.93	3.88	^{152}Sm	5.05	5.08	5.09
^{65}Cu	3.91	3.95	3.89	^{154}Sm	5.07	5.11	5.13
^{64}Zn	3.92	3.97	3.92	^{154}Gd	5.09	5.11	5.12
^{66}Zn	3.94	3.98	3.93	^{156}Gd	5.12	5.14	5.07
^{68}Zn	3.95	4.00	3.96	^{158}Gd	5.13	5.15	5.17
^{70}Zn	3.99	4.00	3.99	^{165}Ho	5.22	5.22	5.21
^{70}Ge	4.03	4.06	4.04	^{166}Er	5.23	5.24	5.24
^{72}Ge	4.05	4.08	4.06	^{174}Yb	5.31	5.30	5.41
^{74}Ge	4.07	4.09	4.07	^{176}Yb	5.31	5.31	5.37
^{76}Ge	4.07	4.10	4.08	^{175}Lu	5.31	5.31	5.37
^{88}Sr	4.23	4.28	4.19	^{181}Ta	5.34	5.36	5.48
^{89}Y	4.26	4.30	4.24	^{184}W	5.36	5.37	5.43
^{90}Zr	4.28	4.32	4.26	^{186}W	5.37	5.38	5.40
^{91}Zr	4.29	4.33	4.31	^{192}Os	5.39	5.41	5.41
^{92}Zr	4.29	4.34	4.29	^{196}Pt	5.41	5.44	5.38
^{94}Zr	4.31	4.36	4.31	^{197}Au	5.43	5.45	5.31
^{96}Zr	4.36	4.40	4.40	^{203}Tl	5.46	5.48	5.46
^{93}Nb	4.32	4.36	4.32	^{205}Tl	5.47	5.49	5.47
^{92}Mo	4.32	4.36	4.29	^{204}Pb	5.49	5.50	5.48
^{94}Mo	4.34	4.38	4.33	^{206}Pb	5.49	5.51	5.49
^{96}Mo	4.35	4.40	4.36	^{207}Pb	5.49	5.51	5.50
^{98}Mo	4.40	4.44	4.39	^{208}Pb	5.50	5.52	5.50
^{100}Mo	4.45	4.47	4.43	^{209}Bi	5.51	5.53	5.52
^{104}Pd	4.49	4.53	4.44	^{232}Th	5.74	5.77	5.70
^{106}Pd	4.51	4.55	4.47	^{238}U	5.80	5.82	5.84
^{108}Pd	4.52	4.57	4.52	-	-	-	-
$\bar{\epsilon}$	0.003	0.035	-	$\epsilon_{\rm rms}$	0.036	0.057	-

comparison with experiment for this question is clearer if decoupled from the problem of static deformation. Looking thus at the Pb and Sn series we see that there seems to be a slight advantage for ETFSI in the former case, while both models work equally well in the latter.

A second general feature of ETFSI as compared to FRDM is that the former tends to produce more easily deformable nuclei. We believe that this behavior results from the inclusion of a correction for spurious rotational energy in the ETFSI calculations, effectively projecting states of good angular momentum out of the deformed wave function. This is not taken into account in FRDM, the resulting error that would arise in deformed nuclei being smoothed over all nuclei in the data fit. Globally, the inclusion of this correction in ETFSI improves the agreement with experiment, but its effect on deformation might well be too strong.

B. Absolute charge radii

We compare in Table II our results for the two models with the data compilation of de Vries *et al.* [28]. When these authors give more than one result we choose the Fourier-Bessel analysis in preference to the Gauss or Fermi parametrizations, while in the case of two or more analyses of the same type we take the mean. Table II also gives the mean error $\bar{\epsilon}$ and the rms error $\epsilon_{\rm rms}$ for each model with respect to these data.

In the case of ETFSI about 20% of the rms error comes from just two nuclei, ^{181}Ta and ^{197}Au. These nuclei are among the worst for the FRDM calculation also, and insofar as the data are reliable it would appear that some essential feature of these nuclei is being missed by both models. However, it is to be noted that all of the quoted experiments for these two nuclei were performed before 1960 (see [28]).

1. ETFSI results

Regardless of this problem, it will be seen that the overall agreement of the ETFSI results with experiment is altogether satisfactory. Indeed, the mean error $\bar{\epsilon}$ is so small that it is difficult to imagine any improvement. Thus it would seem safe to affirm that the ETFSI-1 mass formula satisfies the test of simultaneously optimizing both the fit to the masses and the fit to charge radii with the same parameter set (set SkSC4 of [6]).

Of particular interest in this optimizing set of parameters is the charge-radius constant r_0. The value determined by the mass fit of [6] is $r_0 = 1.140 \pm 0.005$ fm (in [6] this result was expressed in terms of k_F, the Fermi momentum of symmetric nuclear matter at saturation, and the limits were not given); the present work shows that this value optimizes also the charge radii.

TABLE III. Surface diffuseness parameters (fm) in ETFSI-1 calculation (experimental values in parentheses).

	a_p	C_p	$a_{\rm ch}$
^{40}Ca	0.4565	3.74314	0.478 (0.561)
^{58}Ni	0.4498	4.28583	0.481 (0.560)
^{88}Sr	0.4320	4.95013	0.474 (0.496)
^{120}Sn	0.4272	5.52875	0.475 (0.576)
^{206}Pb	0.4216	6.71033	0.477 (0.545)
^{208}Pb	0.4205	6.72724	0.476 (0.549)

Turning now to the diffuseness parameter $a_{\rm ch}$, we limit ourselves to spherical nuclei that have been well measured and fitted to two-parameter Fermi (2pF) charge distributions of the form (1). Our results are given in Table III. In this table a_p and C_p are the parameters that result from the minimization of the ETF energy, while $a_{\rm ch}$ includes the correction for the finite proton size, made as described in the Appendix. The quantity in parentheses is the experimental value of $a_{\rm ch}$, as given in the compilations [28] and [29].

We see that our diffuseness parameters are consistently about 15% too small, which reflects a well-known limitation of the ETF approximation [8]. This error is adequately compensated, as far as binding energies are concerned, by virtue of the fit of the force parameters to the mass data, but the details of the charge distribution are left uncorrected. Clearly, we are approaching here the limits of the ETFSI model.

Nevertheless, it is clear from Eq. (2) that if we ever got both $\langle r^2 \rangle_{\rm ch}^{1/2}$ and $a_{\rm ch}$ right then our value of r_0 would certainly be smaller than the value of 1.14 fm that we gave above. In this connection, it is interesting to note that the HF effective force giving the best fit to electron scattering, the D1 force of the Gogny group [30], has $r_0 = 1.13$ fm, but since no limits have been quoted there is not necessarily any conflict with our own results.

2. FRDM results

The FRDM results shown in Table II have been calculated with the MMST values for all parameters. We see that there is a small but systematic overevaluation of the charge radii, especially for the lighter nuclei, and it is clear that the MMST parameter values are not optimal from the point of view of the charge radii. However, it is not obvious that the MMST values for the parameters r_0 and b are optimal from the point of view of the masses either, since MMST [1] did not vary these parameters in their mass fit, claiming that they were fixed by electron-scattering and muonic x-ray measurements of the charge distribution. Thus it should be possible in principle to improve the FRDM charge-radius predictions simply by readjusting these two nonoptimal parameters. Combining a new value of r_0, most effective in heavy nuclei, with a new value of b, most effective in light nuclei, should permit the elimination of most of the deficiencies remarked in Table II.

First, however, let us see how well the parameter b is in fact determined by the charge-distribution measurements. Examining the 2pF fits of the compilations [28] and [29] we find that we cannot exclude any value of $a_{\rm ch}$ between 0.54 and 0.58 fm, i.e., $b_{\rm ch}$ between 0.98 and 1.05 fm, according to Eq. (3). Now the way in which MMST [1] use the parameter b implies that it must be interpreted as referring to point protons, and we have treated it likewise. We thus estimate that the relevant

range of acceptable b values is 0.93 to 1.00 fm, which means that the MMST choice lies near the upper limit. However, there is some indication in the data (apparent in Table III) of a slight decrease on moving to heavier nuclei, which could be a manifestation of the I-dependent effect revealed by ETF calculations (Sec. II B). Since the FRDM does not take account of this effect, one should show some preference for higher values of b. It is in this sense that we believe the MMST choice for b to be reasonable. But since different measurements of even the same nucleus often show considerable scatter, lower values cannot be excluded.

In Table IV we present the results of three exploratory attempts to fit r_0 and b to the charge-radius data. [In all cases we have checked that the changes of r_0 do not affect the quality of the fit to the isotope chains; $\delta\langle r_{\rm ch}^2\rangle$ is independent of b, as can be seen from Eq. (6).] Fit 1 holds b at its canonical (and, as we have seen, plausible) value of 0.99 fm, and optimizes with respect to r_0. At first sight it would appear that a considerable improvement has been obtained, while reducing the discrepancy between the ETFSI and FRDM values of r_0. However, this fit is still unsatisfactory, since it does not lead to the correct variation of $\langle r_{\rm ch}^2\rangle$ with A, heavy nuclei now being too small, while light nuclei are still too big. In fit 2 we fix r_0 at its ETFSI value of 1.14 fm, and optimize with respect to b. We see that this is the worst of our fits, and that the required value of b is rather high. Thus, it is unlikely that we can reconcile the FRDM and ETFSI values of r_0 in this way. The best fit, fit 3, obtained by releasing both parameters, is no better than the ETFSI fit, in which no parameter adjustment was made at all. Furthermore, the value $b = 0.83$ fm is probably too low.

We stress the exploratory nature of these fits of the parameters r_0 and b. Our main conclusion here is that from the standpoint of charge radii the MMST values of r_0 and b are far from optimal. But in making a new fit it should be borne in mind that in the MMST mass fit r_0 and b were not the only parameters that were not optimized: The macroscopic parameter L of the FRDM was arbitrarily set equal to zero, even though it influences radii through the quantity $\bar{\delta}$ of Eq. (10). Furthermore, if any of these parameters r_0, b, or L in the mass fits are changed there will be changes in the other parameters as well, and thus changes in the calculated radii. Such an undertaking is clearly beyond the scope of the present paper.

Nevertheless, it is of interest to note in this respect the role of the surface-stiffness parameter Q, an increase of which leads to an increase in the sharp proton radius R_Z of Eq. (10), through a reduction in the neutron-skin thickness [second term on the right-hand side of Eq. (10)]. Thus it might be possible to improve the agreement between the FRDM radii and experiment by taking a lower value of r_0 and a higher value of Q. In this way one would reduce the discrepancy between the ETFSI and FRDM models not only for r_0 but also for Q, the two models giving in their present form 112.3 MeV and 29.4 MeV, respectively, as noted above.

TABLE IV. Fit of FRDM parameters to charge-radius data.

Fit	r_0	b	$\bar{\epsilon}$	$\epsilon_{\rm rms}$
1	1.15	0.99	0.003	0.049
2	1.14	1.03	-0.001	0.056
3	1.18	0.83	0.000	0.035

IV. CONCLUDING REMARKS

In this paper we have examined two modern mass formulas, the ETFSI formula and the FRDM formula, from the point of view of charge radii. The object is to see whether with all parameters being determined by the mass fit, the fit to the charge radii is simultaneously optimized. In this way the coherence of the underlying physics of the models can be tested.

The results of Sec. III A on the variation of charge radii along isotope chains shows that both of these microscopic-macroscopic models work fairly well, even though in both cases the radius is determined entirely by the macroscopic density distribution. Indeed, it seems that the major role of the microscopic corrections is to drive the deformation, to which extent they do show up in the calculated radius. For some chains the ETFSI model works better than the FRDM model, while in other chains the contrary situation prevails. It is not possible to say that one model is better than the other as far as the variation of the charge radii along isotope chains is concerned.

As for the absolute values of the rms charge radii (Sec. III B), we have seen that the ETFSI model works well in its present form, and satisfies the criterion of simultaneously optimizing the mass and charge-radius fits with the same parameter set. The situation concerning the FRDM formula is somewhat ambiguous. In the mass fit of MMST [1] certain parameters were not optimized, and we have shown that the choice that was made for these parameters was far from optimal for charge radii. Thus it is still conceivable that the FRDM can be simultaneously optimized to the mass and charge-radius data.

ACKNOWLEDGMENTS

We thank M. Brack for reminding us of the importance of nuclear radii to the mass-formula problem, and S. Das Gupta for skillful handling of communication problems. This work was supported in part by NSERC of Canada.

APPENDIX A: FOLDING THE FINITE PROTON

If we write the charge distribution within the finite proton as $f(|\mathbf{r}-\mathbf{r}'|)$ we have

$$\rho_{\rm ch}(\mathbf{r}) = \int \rho_p(\mathbf{r}') f(|\mathbf{r}-\mathbf{r}'|) d^3\mathbf{r}'. \tag{A1}$$

Then if we take the Gauss form

$$f(x) = (\sigma\sqrt{\pi})^{-3} \exp\left(-\frac{x^2}{\sigma^2}\right) \tag{A2}$$

for the charge distribution within the proton, rms radius $s = \sqrt{\frac{3}{2}}\sigma$, we have for a spherical distribution of protons

$$\rho_{\rm ch}(r) = \frac{2}{\sigma\sqrt{\pi}}\frac{1}{r}e^{-r^2/\sigma^2}\int dr' r' \rho_p(r') e^{-r'^2/\sigma^2}\sinh\frac{2rr'}{\sigma^2} \ . \tag{A3}$$

To fit this folded distribution to a Fermi function we calculate the Ford-Wills moments

$$R_k = \left\{\frac{k+3}{3}\langle r^k\rangle\right\}^{1/k} \ , \tag{A4}$$

where

$$\langle r^k\rangle = \frac{\int r^{k+2}\rho_{\rm ch}(r)dr}{\int r^2\rho_{\rm ch}(r)dr} \ , \tag{A5}$$

and use the fact that for a Fermi distribution one has

$$R_k = C + \frac{\pi^2}{6}(k+5)\frac{a^2}{C} \ . \tag{A6}$$

The rms radius of the resulting Fermi distribution is then found to satisfy Eq. (5), i.e., Eq. (16) of [9], to a high degree of precision.

On the other hand, Eqs. (17)–(18) of [9] relate the surface diffuseness of this folded distribution to that of the original distribution of point protons by

$$a_{\rm ch}^2 - a_p^2 = \frac{s_p^2}{\pi^2} \ . \tag{A7}$$

We find this difference to be about double the value given by the folding procedure. Presumably, the approximations made in [9] are not valid for such small quantities, and we accordingly do not make use of Eq. (A7).

[1] P. Möller, W. D. Myers, W. J. Swiatecki, and J. Treiner, At. Data Nucl. Data Tables **39**, 225 (1988).

[2] P. Möller, J. R. Nix, W. D. Myers, and W. J. Swiatecki (unpublished).

[3] A. K. Dutta, J.-P. Arcoragi, J. M. Pearson, R. Behrman, and F. Tondeur, Nucl. Phys. **A458**, 77 (1986).

[4] F. Tondeur, A. K. Dutta, J. M. Pearson, and R. Behrman, Nucl. Phys. **A470**, 93 (1987).

[5] J. M. Pearson, Y. Aboussir, A. K. Dutta, R. C. Nayak, M. Farine, and F. Tondeur, Nucl. Phys. **A528**, 1 (1991).

[6] Y. Aboussir, J. M. Pearson, A. K. Dutta, and F. Tondeur, Nucl. Phys. **A549**, 155 (1992).

[7] E .W. Otten, in *Treatise on Heavy-Ion Science*, edited by D. A. Bromley (Plenum, New York, 1988), Vol. 8, p. 515, and references therein.

[8] M. Brack, C. Guet, and H.-B. Håkansson, Phys. Reports **123**, 275 (1985).

[9] W. D. Myers, Nucl. Phys. **A204**, 465 (1973).

[10] Y. Aboussir, J. M. Pearson, A. K. Dutta, and F. Tondeur (unpublished).

[11] W. D. Myers and K.-H. Schmidt, Nucl. Phys. **A410**, 61 (1983).

[12] F. Buchinger, E. B. Ramsay, E. Arnold, W. Neu, R. Neugart, K. Wendt, R. E Silverans, P. Lievens, L. Vermeeren, D. Berdichevsky, R. Fleming, D. W. L. Sprung, and G. Ulm, Phys. Rev. C **41**, 2883 (1990).

[13] P. Lievens, L. Vermeeren, R. E. Silverans, E. Arnold, R. Neugart, K. Wendt and F. Buchinger, Phys. Rev. C **46**, 797 (1992).

[14] P. Lievens, R. E. Silverans, L. Vermeeren, W. Borchers, W. Neu, R. Neugart, K. Wendt, F. Buchinger, and E. Arnold, Phys. Lett. B **256**, 141 (1991).

[15] W. Borchers, E. Arnold, W. Neu, R. Neugart, K. Wendt, and G. Ulm, Phys. Lett. B **216**, 7 (1989).

[16] Th. Hilberath, St. Becker, G. Bollen, H.-J. Kluge, U. Krönert, G. Passler, J. Rikovska, and R. Wyss, Z. Phys. A **342**, 1 (1992).

[17] U. Dinger, J. Eberz, G. Huber, R. Menges, R. Kirchner, O. Klepper, T. Kühl, and D. Marx, Nucl. Phys. **A503**, 331 (1989).

[18] G. D. Alkhazov, A. E. Barzakh, V. P. Denisov, V. S. Ivanov, I. Ya.Chubukov, N. B. Buyanov, V. S. Letokhov, V. I. Mishin, S. K. Sekatsky, and V. N. Fedoseev, *Proceedings of the Fifth International Conference on Nuclei far from Stability*, Rosseau Lake, Ontario, 1987, edited by I. S. Towner, AIP Conf. Proc. No. 164 (AIP, New York, 1988), p. 115; Academy of Science of the USSR, Leningrad Nuclear Physics Institute, Report No. 1309, 1987 (unpublished).

[19] S. Frauendorf and V. V. Pashkevich, Phys. Lett. **55B**, 365 (1975).

[20] I. Ragnarsson, in *Future Directions in Studies of Nuclei Far From Stability*, edited by J. H. Hamilton, E. H. Spejewski, C. R. Bingham, and E. F. Zganjar (North Holland, Amsterdam, 1980), p. 367.

[21] P. Bonche, J. Dobaczewski, H. Flocard, and P.-H. Heenan, Nucl. Phys. **A530**, 149 (1991).

[22] H. Mach, F. K. Wohn, G. Molnar, K. Sistemich, J. C. Hill, M. Moszynski, R. L. Gill, W. Krips, and D. S. Brenner, Nucl. Phys. **A523**, 197 (1991).

[23] S. Raman, C. H. Malarkey, W. T. Milner, C. W. Nestor, Jr., and P. H. Stelson, At. Data Nucl. Data Tables **36**, 1 (1987).

[24] W. D. Myers and P. Rozmej, Nucl. Phys. **A470**, 107 (1987).

[25] G. A. Leander, R. K. Sheline, P. Möller, P. Olanders, I. Ragnarsson, and A. J. Sierks, Nucl. Phys. **A388**, 452 (1982).

[26] W. Nazarewicz, P. Olanders, I. Ragnarsson, J. Dudek, G. A. Leander, P. Möller, and E. Ruchowska, Nucl. Phys. **A429**, 269 (1984).

[27] D. Berdichevsky and F. Tondeur, Z. Phys. A **322**, 141 (1985).

[28] H. de Vries, C. W. de Jager, and C. de Vries, At. Data Nucl. Data Tables **36**, 495 (1987).

[29] C. W. de Jager, H. de Vries, and C. de Vries, At. Data Nucl. Data Tables **14**, 479 (1974).

[30] J. Dechargé and D. Gogny, Phys. Rev. C **21**, 1568 (1980).